Bull. Mater. Sci., Vol. 39, No. 3, June 2016, pp. 627–632. © Indian Academy of Sciences.
DOI 10.1007/s12034-016-1210-2

Structural studies of $Nd_{1.85}Ce_{0.15}CuO_4$ + Ag superconducting system

N RADHIKESH RAVEENDRAN[1,3], A K SINHA[2,3], R RAJARAMAN[1,3], M PREMILA[1], E P AMALADASS[1], K VINOD[1], J JANAKI[1,3,*], S KALAVATHI[1] and AWADHESH MANI[1,3]

[1]Materials Science Group, Indira Gandhi Centre for Atomic Research, Kalpakkam 603102, India
[2]Indus Synchrotron Utilization Division, Raja Ramanna Centre for Advanced Technology, Indore 452013, India
[3]Homi Bhabha National Institute, Training School Complex, Mumbai 400085, India

MS received 24 November 2015; accepted 20 January 2016

Abstract. **We have studied for the first time the effect of Ag addition (0–15 wt%) to the superconducting system, $Nd_{1.85}Ce_{0.15}CuO_4$, on its crystal structure and local structural features, using synchrotron X-ray diffraction (SXRD) and Raman spectroscopy, respectively. SXRD and subsequent Rietveld refinement studies on powders of $Nd_{1.85}Ce_{0.15}CuO_4$ + Ag system indicate a small but significant change in lattice parameter upon Ag addition, showing evidence for possible incorporation of Ag to the extent of ∼1 wt%. Raman spectroscopic studies indicate that the parent structure of $Nd_{1.85}Ce_{0.15}CuO_4$ remains unaffected with no major local structural changes on doping with silver. However, all Raman modes show minor phonon hardening upon Ag addition, which is consistent with the unit cell volume reduction as is observed in XRD. A systematic bleaching out of the apical oxygen defect mode was also observed with increased Ag addition. Polarized Raman measurements helped to identify the asymmetric nature of the B_{1g} Raman mode. X-ray diffraction studies on pellets of $Nd_{1.85}Ce_{0.15}CuO_4$ + Ag system further indicate a randomization of preferred orientation upon Ag addition. The superconductivity of the $Nd_{1.85}Ce_{0.15}CuO_4$ + Ag system has been well characterized for all the compositions studied.**

Keywords. **Cuprate superconductors; structural studies; Raman spectroscopy.**

1. Introduction

The effect of silver addition on ceramic superconductors is a topic of current interest [1–5]. This is because the fabrication of cuprate superconductor wires and tapes is usually carried out using silver as cladding. Generally, silver is considered a nonreactive element, however, sometimes it can also substitute for copper which is quite unusual and interesting [1,2]. Apart from the possibility of a small amount of silver (Ag) dissolving in the lattice, the increased concentration of Ag (5–15 wt%) can regulate the dynamics of the sintering/re-crystallization process and as a result determine the physical nature of the inter- and intra-grain fluxon drift motion, thereby affecting the superconducting critical current density. Studies on the introduction of silver into high-Tc-superconductors like Bi–Pb–Sr–Ca–Cu–O and $YBa_2Cu_3O_7$ have revealed that Ag is found to improve their structural and superconducting properties [3–5]. It has been reported that silver promotes the *c*-axis orientation and crystallization of the superconducting [3] phase and catalyzes the inter-granular coupling of the superconducting grains. Ag addition also leads to the enhancement of critical current density of almost all bulk high temperature superconductors including the rare earth cuprates, MgB_2 and rare earth iron pnictides, mainly due to an improvement in inter-granular coupling [6–8]. Moreover, Ag is also an established additive for improving mechanical properties of cuprate superconductors [9]. However, the effect of Ag addition on the electron-doped superconductor, $Nd_{1.85}Ce_{0.15}CuO_4$ has not been reported yet. In this paper, the results of a structural study of the $Nd_{1.85}Ce_{0.15}CuO_4$ + Ag system through X-ray diffraction (XRD) and Raman spectroscopy are presented.

2. Experimental

The synthesis of $Nd_{1.85}Ce_{0.15}CuO_4$ + Ag (0, 5, 10 and 15 wt%) polycrystalline pellets has been carried out by first synthesizing $Nd_{1.85}Ce_{0.15}CuO_4$ by solid-state reaction and then mixing required quantities of pure Ag powder (99.9% pure) and $Nd_{1.85}Ce_{0.15}CuO_4$ powder, repeated homogenizing and annealing and finally, sintering at 860°C for 24 h. This is followed by annealing under argon at 890°C to induce superconductivity.

The structural features of the composite system, $Nd_{1.85}Ce_{0.15}CuO_4$ + Ag have been probed by synchrotron X-ray diffraction and Raman spectroscopy. The synchrotron X-ray diffraction measurements have been done on finely ground powders of $Nd_{1.85}Ce_{0.15}CuO_4$ + Ag in the beam line BL-12 (ADXRD beam line) at INDUS-II synchrotron source at Raja Ramanna Centre for Advanced Technology, Indore, India. XRD patterns were recorded on a MAR3450 image plate and the sample was mounted on Debye–Scherrer geometry. The 2D ring pattern recorded on the image plate was converted

*Author for correspondence (jjanaki@igcar.gov.in)

to 2 theta (2θ) *vs.* intensity (I) plots, using FIT2D program [10]. The wavelength and sample to detector distance were accurately calibrated by using XRD pattern of LaB_6 NIST standard. The Rietveld analysis of the XRD data (wavelength = 0.665422 Å) was performed using GSAS-EXPGUI software [11]. An XRD study of the pellets has also been carried out to establish the orientation using a laboratory powder diffractometer (D500 STOE using CuKα radiation, operated with a power of 40 kV and 30 mA, in the Bragg–Brentano geometry).

Raman spectroscopic measurements have been carried out on pellets of $Nd_{1.85}Ce_{0.15}CuO_4$ and $Nd_{1.85}Ce_{0.15}CuO_4$ + Ag using Renishaw InVia micro Raman spectrometer (Renishaw, UK) using 10 mW power of 514.5 nm Ar ion laser. Measurements were made in the backscattering geometry with Z axis of laboratory frame taken as direction of laser propagation and the sample surface as the XY plane. Polarized Raman measurements were carried out by inserting an analyzer and an additional half wave plate in scattered light path for parallel polarization (XX) and perpendicular polarization (XY), respectively. Data analysis was carried out using WIRE software of the Renishaw make inVia Raman spectrometer. Collected spectra were smoothed and corrected for background. Additional area normalization was done for unpolarized spectra, while no further processing was done for polarized spectra. Un-polarized Raman spectra were fitted with Lorentzian line shapes for the observed main modes.

Characterization of superconductivity has been carried out using low temperature electrical resistivity and magnetization measurements in the temperature range of 4–300 K. The resistivity data have been obtained by the four probe method using Vander Pauw technique. DC magnetization characterization has been carried out using a Cryogenic make liquid helium-based vibrating sample magnetometer.

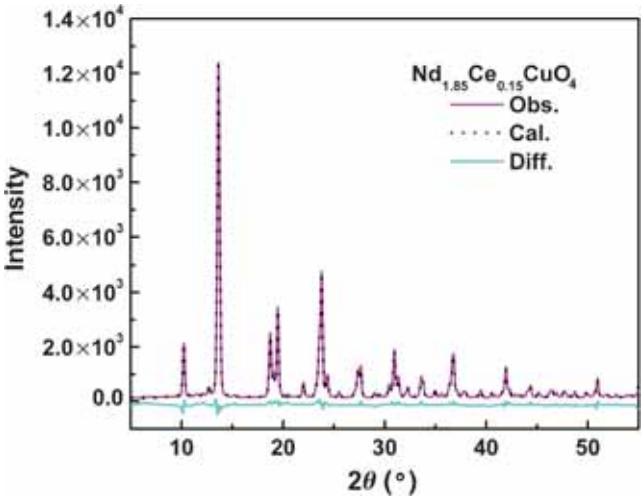

Figure 1. Rietveld refined powder XRD plot of $Nd_{1.85}Ce_{0.15}CuO_4$.

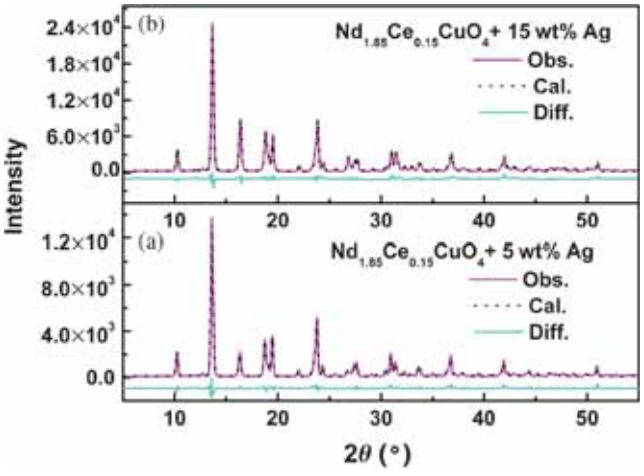

Figure 2. Rietveld refined powder XRD plot of (**a**) $Nd_{1.85}Ce_{0.15}CuO_4$ + 5 wt% Ag and (**b**) $Nd_{1.85}Ce_{0.15}CuO_4$ + 15 wt% Ag.

3. Results and discussion

To investigate the overall distribution of silver in the inter- and intra-granular regions and also to precisely determine the changes in lattice constants upon Ag addition, the synchrotron XRD analysis and Rietveld refinement have been undertaken. The Rietveld refinement plots of the $Nd_{1.85}Ce_{0.15}CuO_4$–Ag system (Ag = 0, 5 and 15 wt%) are presented in figures 1 and 2a,b, respectively. The background function used is the Chebyshev polynomial of the first kind as given in the GSAS programme. The refinement has been carried out in sequence: background, scale factor, lattice parameters, profile parameters, phase fractions and thermal vibration parameters.

The lattice parameters and Ag content for the samples are listed in table 1. The quantitative phase information is obtained assuming that the weight fraction W_p of the p-th phase in a mixture is given by [12] $W_p = S_p Z_p M_p V_p / \sum_i S_i Z_i M_i V_i$; where S_p, M_p, Z_p, V_p are the refined Rietveld scale factor, the mass of the formula unit, the number of formula units per unit cell and the unit cell volume, respectively, of the phase p. The summation in the denominator accounts for all crystalline phases in this case including $Nd_{1.85}Ce_{0.15}CuO_4$ and Ag.

The results of Rietveld refinement studies of $Nd_{1.85}Ce_{0.15}CuO_4$ + Ag system (table 1) indicate a small but significant change in lattice parameter upon Ag addition (c lattice parameter decreases from 12.085 to 12.065 Å for the system $Nd_{1.85}Ce_{0.15}CuO_4$ + Ag upon increasing Ag from 0 to 15%). This is associated with a very small decrease in the concentration of free silver by around 1% (our estimated composition of the sample is $Nd_{1.85}Ce_{0.15}CuO_4$ + 14% Ag compared to the nominal composition for the sample $Nd_{1.85}Ce_{0.15}CuO_4$ + 15% Ag) showing evidence for possible incorporation of Ag in the lattice to the extent of roughly 1 wt%. As it is well known that Ag takes 1+ and 3+ oxidation states and Ag^{3+} ion has an ionic radius 0.81 Å comparable to 0.688 Å for Cu^{2+}, it perhaps substitutes Cu ion. This may lead to additional electron doping similar to Ce^{4+} and consequent reduction of c lattice parameter, perhaps due to removal of apical oxygen defects upon electron doping

Table 1. Structural parameters refined from synchrotron XRD data and estimated Ag content from quantitative XRD analysis of $Nd_{1.85}Ce_{0.15}CuO_4$ + Ag system for compositions as indicated.

Nominal composition	Lattice parameter		Unit cell volume (Å^3)	Silver content	
	'a', Å (±0.0002)	'c', Å (±0.0005)		Phase fraction	Sph weight %
$Nd_{1.85}Ce_{0.15}CuO_4$	3.948	12.085	188.365		
$Nd_{1.85}Ce_{0.15}CuO_4$ + 5% Ag	3.947	12.082	188.22	0.2801	5.2
$Nd_{1.85}Ce_{0.15}CuO_4$ + 15% Ag	3.940	12.065	187.29	0.7445	13.9

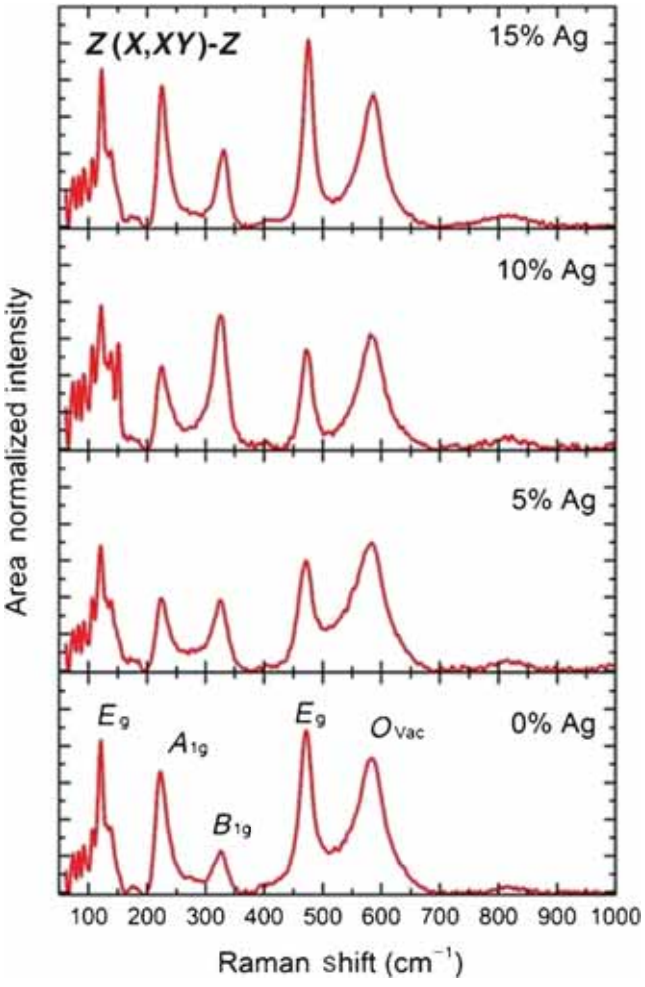

Figure 3. Raman spectra of the $Nd_{1.85}Ce_{0.15}CuO_4$ + Ag (0, 5, 10 and 15 wt%) pellets.

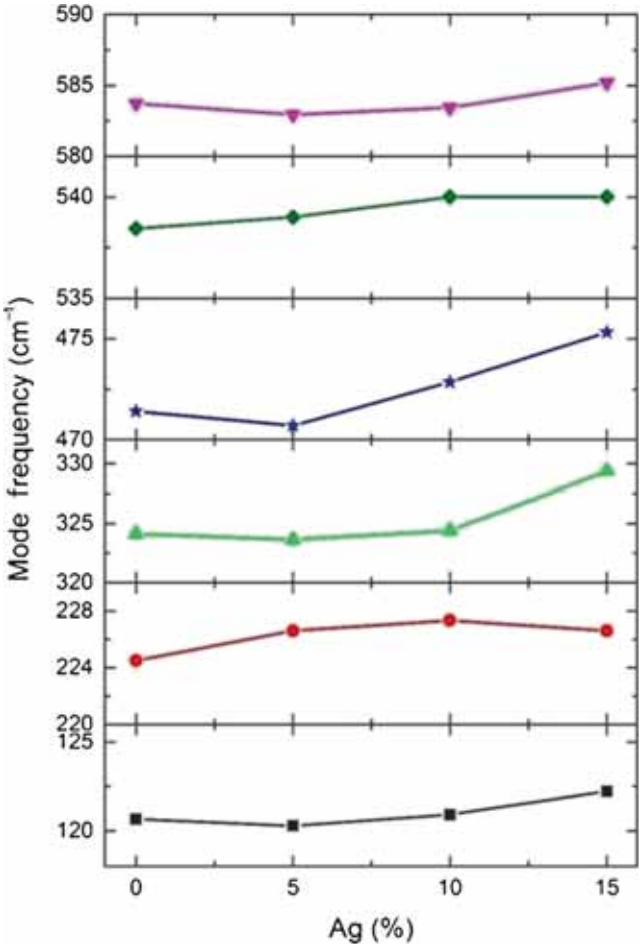

Figure 4. Variation of mode frequencies with increasing Ag addition.

(reduction of Cu^{2+}). A very slight Ag doping for Cu established for the $YBa_2Cu_3O_7$ superconducting system [1] gives evidence for the possibility of a small but finite substitution of Ag for Cu in the cuprate superconductors.

Raman spectroscopic studies have been carried out to probe the local structural changes, oxygen disorder and preferred-orientation effects associated with the addition of Ag to $Nd_{1.85}Ce_{0.15}CuO_4$. The room temperature is unpolarized $Z(X, XY)$-Z and area normalized Raman spectra of $Nd_{1.85}Ce_{0.15}CuO_4 + x$Ag ($x$ = 0, 5, 10 and 15%) system are presented in figure 3. Intensity axis limits are kept equal for all spectra to compare relative intensity variations. The low energy Raman spectra below 700 cm^{-1} exhibit five sharp phonon modes and a weak mode around 820 cm^{-1}, which may arise from two phonon scattering [13]. The sharp spectral feature at 223 cm^{-1} may be attributed in analogy with existing literature on the Raman response of $Nd_{1.85}Ce_{0.15}CuO_4$ [14], to the crystal field excitations of the Nd^{3+} ion along Z direction (A_{1g}). The sharp feature at 326 cm^{-1} is a B_{1g} phonon associated with the out-of-phase c axis vibration of the oxygen atoms in the CuO_2 plane and the peak around 480 cm^{-1} is associated with the in-phase vibration of the oxygen atoms in the CuO_2 plane with E_g symmetry [15]. The origin of the broad feature at 580 cm^{-1} may be a defect mode arising due to apical oxygen atoms in

excess of O_4 and has been widely reported in literature [13–17]. In addition, a very broad satellite feature at 540 cm^{-1} is observed for the pristine (Ag content = 0) sample which is perhaps associated with a wider distribution of apical oxygen defect mode frequencies arising due to a broader distribution of the oxygen defects at interstitial sites. Apart from these major modes, a sharp mode at ∼120 cm^{-1} is observed in all samples. This mode is an E_g symmetry mode of $Nd_{1.85}Ce_{0.15}CuO_4$ analogous to the 480 cm^{-1} E_g Raman mode [17].

The set of unpolarized Raman spectra for $Nd_{1.85}Ce_{0.15}CuO_4$ and $Nd_{1.85}Ce_{0.15}CuO_4$ + Ag samples are shown in figure 3. The modes were fitted with Lorentzian line shapes. Figure 4 shows the variation of mode frequencies with increase in Ag addition. As seen from the figure, all modes show slight hardening with increase in Ag content. This is consistent with the unit cell volume reduction observed with increasing Ag addition, as shown in table 1.

Figure 5 shows variation of area under O-defect modes at 540 and 580 cm^{-1}, while the defect mode corresponding to 580 cm^{-1} shows a reduction, the 540 cm^{-1} mode is also reducing in intensity and nearly diminishes with increasing Ag content. This may be due to partial removal of some of the apical oxygen present in excess of O_4 by Ag defects, which could lead to a shrinking of the c lattice constant as observed. Influence of Ag addition on intensities of observed modes could not be analysed owing to the strong polarization effects, arising from orientation of few grains sampled in the micron size laser spot. The incident laser of ∼1 μm spot diameter is linearly polarized and aligned in X direction of the laboratory frame. Considering the polycrystalline nature of the samples, Raman signal is expected to be arising from randomly oriented crystals. However, the small area probed by the laser spot can still introduce orientation-induced polarization effects on the observed intensities of Raman active modes. This was indeed confirmed by measurements done at various spots with different grain sizes, which showed varied intensities of observed modes for same sample (plots not shown).

We have carried out polarized Raman spectroscopic studies of the pristine $Nd_{1.85}Ce_{0.15}CuO_4$ as well as Ag-doped samples. Figure 6 compares the Raman spectra of both parallel (XX) and perpendicular (XY) polarized scattering. Except B_{1g} mode at 325 cm^{-1}, all other modes show drastic reduction in intensity for perpendicular polarization, implying near symmetric nature of these modes. It is interesting to note that the B_{1g} mode shows non-monotonous behaviour with increasing intensity up to 10% of Ag addition and decrease in intensity for 15%, indicating possible influence of Ag addition in altering local structure. However, present Raman measurements on polycrystalline samples suffer from orientation-induced polarization effects on the observed intensities of other Raman active modes, which prevent us from interpreting the possible influence of Ag on the local structure or bonding. Further evidence is required from

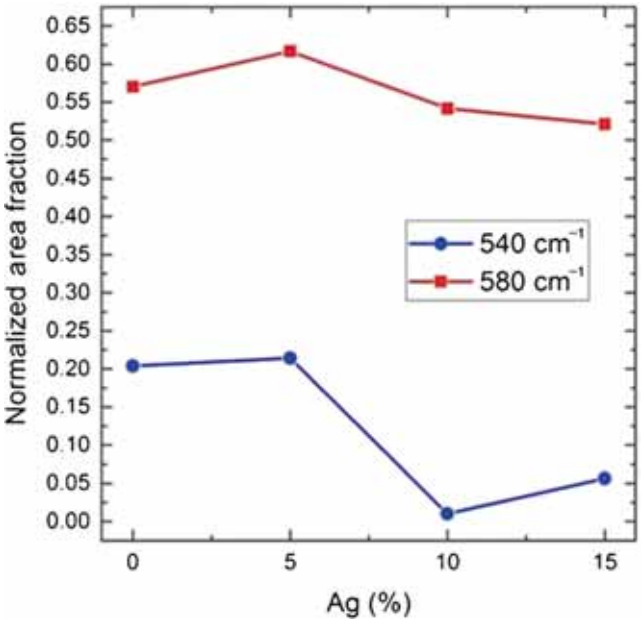

Figure 5. Variation of normalized area under 540 and 580 cm^{-1} O-defect modes as a function of Ag content.

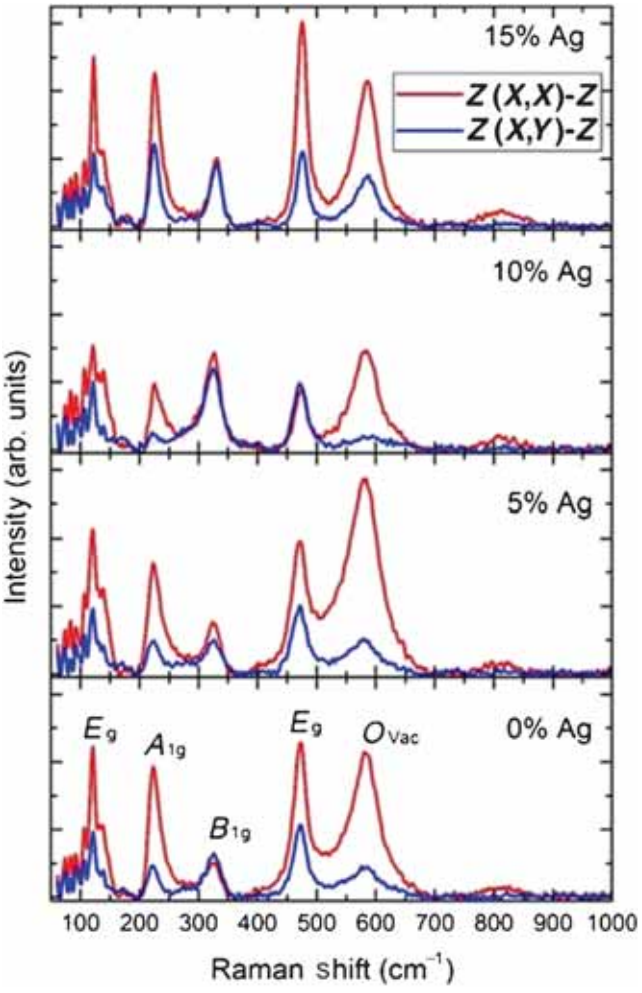

Figure 6. Polarized Raman scattering spectra of both parallel (X, X), indicated by red lines and perpendicular (X, Y), indicated by blue lines.

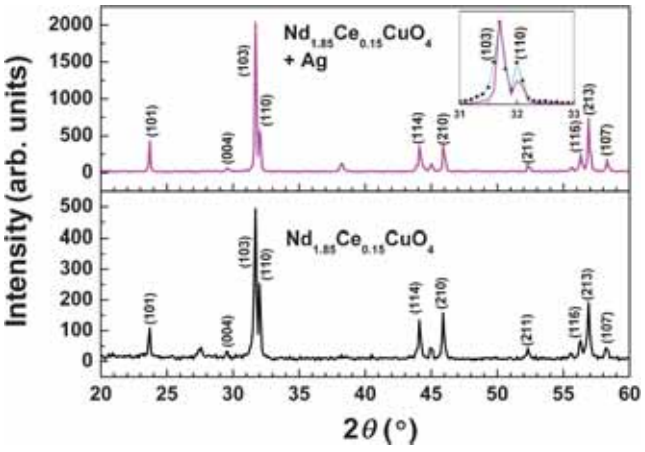

Figure 7. XRD patterns of the $Nd_{1.85}Ce_{0.15}CuO_4$ + Ag (0 and 5 wt%) pellets. Inset shows the intensity comparison of the (103) and (110) reflections for Ag 5% (solid) *vs.* Ag 0% (dot).

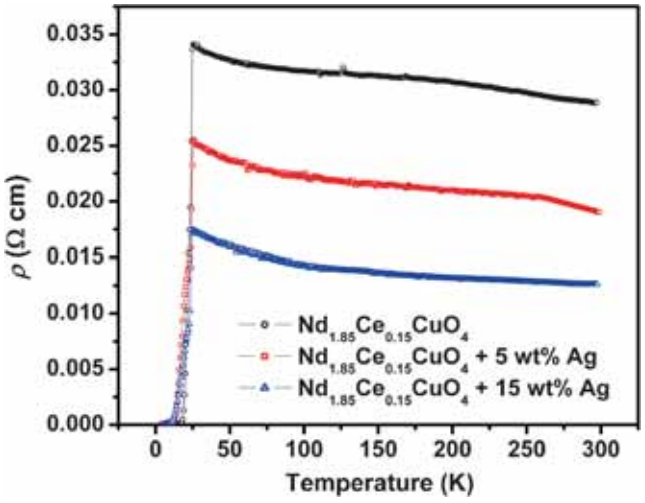

Figure 8. Variation of electrical resistivity of the $Nd_{1.85}Ce_{0.15}CuO_4$ + Ag (0, 5 and 15 wt%) system between 4.2 and 300 K.

Raman studies on single crystalline or epitaxial films of Ag-doped NCCO with corroborating studies using XRD and extended X-ray absorption fine structure (EXAFS).

To establish possible changes of crystallographic-preferred orientation upon Ag addition to the system, XRD patterns of $Nd_{1.85}Ce_{0.15}CuO_4$ + Ag (0 and 5%) pellets have been recorded. They have been presented in figure 7. The data have been analysed with respect to intensity ratio variations. Figure 7 (inset) highlights the reduction in intensity of the (110) reflection upon Ag addition, indicating a randomization of the small degree of preferred orientation initially present in the pristine $Nd_{1.85}Ce_{0.15}CuO_4$ sample.

Superconducting property of the system has been investigated by low temperature electrical resistivity and magnetization measurements in the temperature range 4–300 K. They indicate systematic changes in resistive and magnetic behaviour upon Ag addition. Figure 8 presents the electrical resistivity *vs.* temperature data. The onset temperature of

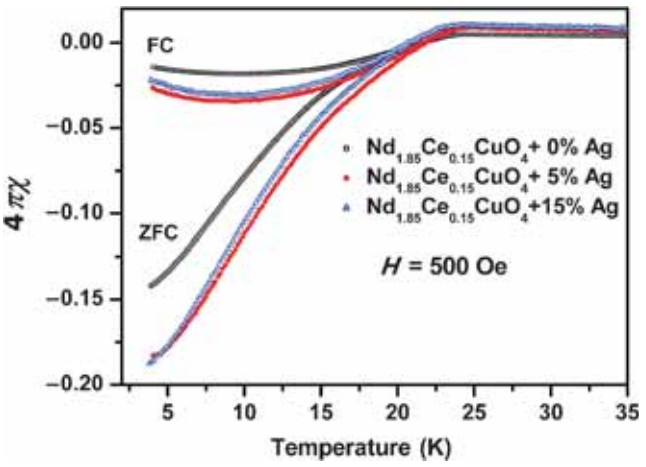

Figure 9. DC magnetization measurements of the $Nd_{1.85}Ce_{0.15}CuO_4$ + Ag (0, 5 and 15 wt%) system between 4 and 30 K for zero field-cooled (ZFC) and field-cooled (FC) conditions, under a field of 500 Oe.

superconductivity of all the samples is 24 K. The resistivity decreases with increasing silver content as expected. Further characterization of superconductivity using DC magnetization is presented in figure 9. The magnetization measurements have been carried out under zero field-cooled (ZFC) and field-cooled (FC) conditions for a measuring field of 500 Oe. The difference in values of magnetization in ZFC and FC arises due to trapped flux during FC. The onset temperature of superconductivity of all the samples is 23.5 K in close agreement with the magnetization data. The diamagnetic shielding increases with Ag content.

4. Conclusions

The effects of Ag addition on the electron-doped cuprate, $Nd_{1.85}Ce_{0.15}CuO_4$ is investigated for the first time. The studies have essentially focussed on the crystal structure and local structural features of the $Nd_{1.85}Ce_{0.15}CuO_4$ + Ag composite system by SIXRD and Raman spectroscopy. In addition, quantitative estimation of available free silver has been carried out. The observed small but significant change in lattice parameter upon Ag addition is an evidence for possible incorporation of Ag to the extent of ∼1 wt% with the rest of the silver present as free silver, perhaps at the grain boundaries, as estimated quantitatively. The reduction in unit cell volume upon Ag addition is consistent with the minor phonon hardening of all Raman modes observed in this study. Other interesting changes observed in structural features upon Ag addition include a diminishing of the apical oxygen defect mode as well as a randomization of preferred orientation.

References

[1] Zhang and Chongmin 1991 Thesis, University of British Columbia

[2] Malik S K, Tomy C V, Umarji A M, Adroja D T, Ram Prasad N C, Soni A Mohan *et al* 1987 *J. Phys. C Solid State Phys.* **20** L417

[3] Srinivas B and Subba Rao G V 1992 *Bull. Mater. Sci.* **15** 403

[4] Dhananjay Kumar M, Sharon P R, Apte R, Pinto S P, Pai S C, Purandare C P *et al* 1994 *J. Appl. Phys.* **76** 1349

[5] Poonam Rani, Rajveer Jha and Awana V P S 2013 *J. Supercond. Novel Magn.* **26** 2347

[6] Chen D-X, Shi Y-H, Navau C, Sanchezand A and Cardwell D A 2012 *Supercond. Sci. Technol.* **25** 014010

[7] Kumar D, Pennycook S J, Narayan J, Wang H and Tiwari A 2003 *Supercond. Sci. Technol.* **16** 455

[8] Rani Poonam, Hafiz A K and Awana V P S 2016 *Physica C* **520** 1

[9] Shi Y-H, Dennis A R and Cardwell D A 2015 *Supercond. Sci. Technol.* **28** 035014

[10] Hammersley A P, Svensson S O, Hanfland M, Fitch A N and Hausermann D 1996 *High Pres. Res.* **14** 235

[11] Toby B 2001 *J. Appl. Crystallogr.* **34** 210

[12] Hill R J and Howard C J 1987 *J. Appl. Cryst.* **20** 467

[13] Sugai S and Hidaka Y 1991 *Phys. Rev. B* **44** 809

[14] Jandl S, Iliev M, Thomsen C, Ruf T and Cardona M 1993 *Solid State Commun.* **87** 609

[15] Nathalie Munnikes 2008 Thesis, Technische Universität München

[16] Seongsik Hong, Hyunchul Jo, Hyeonsik Cheong and Gwangseo Park 2005 *Physica C* **418** 28

[17] Popovic Z V, Sakuto A and Balkanski M 1991 *Solid State Commun.* **78** 99